Estimates of observation errors and their correlations in clear and cloudy regions for microwave imager radiances from NWP

Niels Bormann, Alan J. Geer and Peter Bauer

ECMWF, Shinfield Park, Reading
RG2 9AX, United Kingdom
n.bormann@ecmwf.int

ABSTRACT

This contribution provides estimates of effective observation errors and their inter-channel and spatial correlations for microwave imager radiances used in the ECMWF system. The estimates include the error contributions from the observation operator used in the assimilation system. It is investigated how the estimates differ in clear and cloudy/rainy regions. The estimates are obtained using the Desroziers diagnostic.

The results suggest considerable inter-channel and spatial error correlations for current microwave imager radiances with observation errors that are significantly higher than the measured instrument noise. Inter-channel error correlations are even stronger for cloudy/rainy situations, where channels with the same frequency but different polarisations show error correlations larger than 0.9. The findings suggest that a large proportion of the observation error originates from errors of representativeness and errors in the observation operator. The latter includes the errors from the forecast model which can be significant in the case of humidity or cloud and rain.

Assimilation experiments with single SSM/I fields of view highlight how the filtering properties of a 4-dimensional variational assimilation system are changed when inter-channel error correlations are taken into account in the assimilation. Depending on the First Guess departures in the used channels, increments can be larger as well as smaller compared to the use of diagonal observation errors.

1 Introduction

Microwave imager radiances in the ECMWF system are assimilated directly in a 4-dimensional variational (4DVAR) assimilation framework in the "all-sky" system (Bauer et al. 2010, Geer et al. 2010). That is, radiances in clear as well as cloudy or rainy conditions are assimilated, employing a radiative transfer model with scattering parameterisation as required. The system is used operationally for the Special Sensor Microwave Imager (SSM/I, Hollinger et al. 1990) and the Advanced Microwave Scanning Radiometer for the Earth Observing System (AMSR-E, Kawanishi et al. 2003). As is currently common practice, the all-sky system treats the microwave imager radiance errors as independent and assumes a diagonal error correlation matrix.

Observation error covariances, together with background error covariances, play an important role in determining the weight given to an observation in the assimilation. For satellite radiances the assumption of uncorrelated observation errors is questionable, especially as the observation error should include errors from the observation operator and errors of representativeness. The observation operator error includes errors from the radiative transfer and, in the case of strong-constraint 4DVAR, errors in the forecast model used to map from the analysis time to the observation time. Such errrors are expected to be correlated, between channels or spatially.

Estimation of observation error covariances is not straightforward. Nevertheless, a number of methods have been devised, based on First Guess (FG) or analysis departures taken from Numerical Weather Prediction (NWP) systems (e.g., Desroziers et al. 2005, Dee and da Silva 1999, Hollingsworth and

Lönnberg 1986, Rutherford 1972). All of these methods rely on a number of assumptions and these have been summarised in more detail elsewhere (e.g., Bormann and Bauer 2010, Dee and da Silva 1999). Recently, results from three of the methods have been intercompared for sounder radiances used in the ECMWF system (Bormann and Bauer 2010, Bormann et al. 2010). The study showed considerable inter-channel and spatial error correlations for microwave and infrared water vapour or window channel radiances. The results were overall consistent between the three methods applied, even though quantitatively some differences in the estimates were noted, particularly for water vapour channels.

Here we extend the study of Bormann and Bauer (2010) to microwave imager radiances in clear and cloudy conditions. We only apply one of the estimation methods, namely the Desroziers diagnostic (Desroziers et al. 2005). The uncertainties in the observation error estimates found for water vapour radiances in Bormann and Bauer (2010) and Bormann et al. (2010) give some indication on the reliability of our results from just one method. The present contribution is a summary of Bormann et al. (2011).

2 Method and data

2.1 Desroziers diagnostic

The observation error estimates presented here are obtained with the Desroziers diagnostic (Desroziers et al. 2005). This diagnostic assumes that today's variational data assimilation schemes broadly follow linear estimation theory. It assumes that errors have zero bias, and that there are no error correlations between the FG and the observations. In addition, a further assumption is that the weight given to the observations in the analysis is in approximate agreement with the true error covariances. Under these assumptions, the following relationships can be derived in observation space:

$$\tilde{\mathbf{R}} = E\left[\mathbf{d}_a\,\mathbf{d}_b^T\right] \tag{1}$$

$$\mathbf{H}\tilde{\mathbf{B}}\mathbf{H}^T = E\left[\mathbf{d}_b\,\mathbf{d}_b^T\right] - E\left[\mathbf{d}_a\,\mathbf{d}_b^T\right] \tag{2}$$

where $\tilde{\mathbf{R}}$ is the diagnosed observation error covariance matrix, $\tilde{\mathbf{B}}$ is the diagnosed background error covariance matrix, $\mathbf{H}$ is the linearised observation operator, $\mathbf{d}_b$ are the background departures of the observations, $\mathbf{d}_a$ are the analysis departures of the observations, and $E[\,]$ is the expectation operator. Further details on the Desroziers diagnostic and applications of the method can be found in Desroziers et al. (2005) or Bormann and Bauer (2010).

It should be mentioned here that the applicability of the Desroziers diagnostic and its properties in realistic assimilation systems is an area of active research. Recently, Bormann and Bauer (2010) and Bormann et al. (2010) compared results from the Desroziers diagnostic with observation error estimates from two different departure-based methods, and the results were strikingly similar, especially for the estimates of the observation error (σ_o) and the inter-channel error correlations. Estimates for spatial error correlations also showed qualitatively good agreement. However, the study also showed some of the largest differences between methods for water vapour channels, for which it is less clear to separate the FG-departures into a spatially uncorrelated component which can only be observation error and a spatially correlated component which may originate from observation or FG error. While the Desroziers diagnostic does not rely on assuming spatially uncorrelated observation error, such different characteristics of the observation and background errors help for the separability of FG departures into observation and background error contributions. If the length scales of the error correlations are too similar, the method may give misleading results.

Table 1: Channel characteristics of the SSM/I instrument (Hollinger et al. 1990) for the channels used in the assimilation system (For the F-15 SSM/I channel 3 is not used). The instrument noise are measured estimates before the super-obbing employed in the data assimilation system. Also shown are the root mean square (RMS) of the assumed observation error (σ_o) for the clear and the cloudy class (see main text for further details on the definition of these classes).

Channel	Frequency [GHz] and polarisation	Field of view [km × km]	Instrument noise [K]	RMS of assumed clear σ_o [K]	RMS of assumed cloudy σ_o [K]
1 (19V)	19.35 V	69 × 43	0.42	2.1	5.5
2 (19V)	19.35 H	69 × 43	0.45	4.4	10.2
3 (22V)	22.23 V	50 × 40	0.74	2.9	4.1
4 (37V)	37.0 V	37 × 28	0.38	3.5	6.7
6 (85V)	85.5 V	15 × 13	0.73	4.1	6.5

Table 2: As Table 1, but for the AMSR-E instrument (Kawanishi et al. 2003).

Channel	Frequency [GHz] and polarisation	Field of view [km × km]	Instrument noise [K]	RMS of assumed clear σ_o [K]	RMS of assumed cloudy σ_o [K]
5 (19V)	18.7 V	27 × 16	0.55	2.6	7.0
6 (19V)	18.7 H	27 × 16	0.47	6.0	13.2
7 (24V)	23.8 V	32 × 18	0.56	3.0	4.8
8 (24V)	23.8 V	32 × 18	0.54	5.5	9.1
9 (37V)	36.5 V	14 × 8.2	0.51	3.4	6.2

2.2 All-sky assimilation and data used

We present estimates of observation error covariances for SSM/I and AMSR-E. Both are conically scanning microwave imagers, with the specifications for the used channels given in Tables 1 and 2.

The assimilation choices for the all-sky system are described in detail in Geer and Bauer (2010). The all-sky system treats clear and cloudy data in the same framework, calling a radiative transfer model as observation operator which can include a scattering parameterisation if required. Only data over sea within +-60^o latitude are assimilated. Observation biases are corrected using variational bias correction (e.g., Dee 2004). The current choice of observation error model is described in Geer and Bauer (2011). It uses situation-dependent observation errors, assigning observation errors based on the average cloudiness from the observations and the FG. Lower observation errors are used for clear cases, whereas larger ones are used for cloudy/rainy cases (e.g., Tables 1 and 2) . The radiance observations are 'super-obbed' to the Gaussian grid representation of T255 (≈80 km), as described in Geer and Bauer (2010).

While the all-sky system treats clear as well as cloudy cases in the same way, it is useful for diagnostic purposes to separate the observations into clear and cloudy classes. This is done on the basis of an estimate of the liquid water path, using a regression in the 22V (24V in the case of AMSR-E) and 37V brightness temperatures. A threshold of 0.05 kg/m^2 separates the data into roughly equal "clear" and "cloudy/rainy" classes. The classification can be done on the basis of the observations, or on the basis of the FG, leading to four classes. Here, we only consider samples in two of the four classes, that is the class in which the observation and the FG both indicate that the situation is clear, and the class for

which observation and FG both indicate cloud or rain. The reason for this is that the other two classes inherently suffer from sampling biases. For simplicity, we will refer to the two classes just as "clear" and "cloudy" class.

The departure statistics required for the Desroziers diagnostic were taken from an assimilation experiment that covered June and July 2009. It was performed with the ECMWF system (e.g., Rabier et al. 2000), using a T799 (≈25 km) model resolution, an incremental analysis resolution of T255 (≈80 km) and 12-hour 4DVAR. The other observations were as used operationally at the time. All statistics presented here are based on data for the whole of July 2009, using the effective observation departures used in the assimilation system, that is based on super-obbed observations and after bias correction.

3 Results

3.1 Observation errors (σ_o) and their correlations

Estimates of observation errors from the Desroziers diagnostic for the three instruments are shown in Fig. 1. The results for equivalent channels are overall consistent between the three instruments. Estimates for the clear sample are typically between 1-2 K, whereas the cloudy class shows larger error estimates with values typically between 2 and 5 K. Observation error estimates for the cloudy class are expected to be larger due to larger observation operator and representativeness errors (see also Geer and Bauer 2011), and it is reassuring that the results are consistent with this. The estimates are considerably larger than the instrument noise (cf Tables 1 and 2), in particular after the averaging employed in the super-obbing process used in the assimilation. The finding suggests that most of the observation error is due to errors in the observation operator or errors of representativeness.

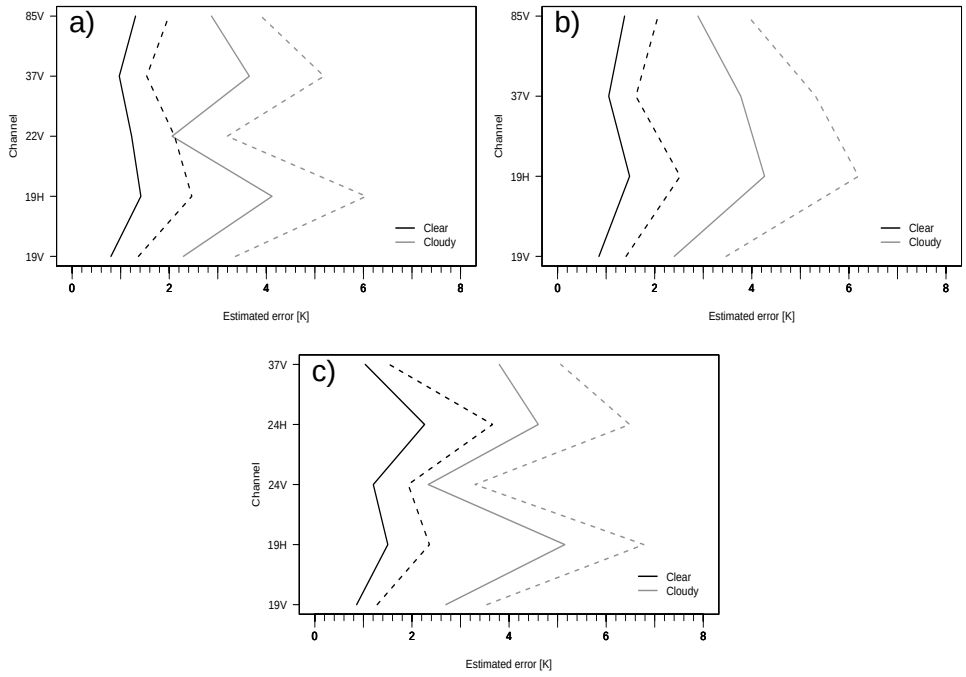

Figure 1: a) Observation error estimates (solid lines) and standard deviations of FG departures (dashed lines) for the F13 SSM/I. Estimates for the clear and the cloudy sample are shown in black and grey, respectively. b) As a), but for the F15 SSM/I. c) As a), but for AMSR-E on Aqua.

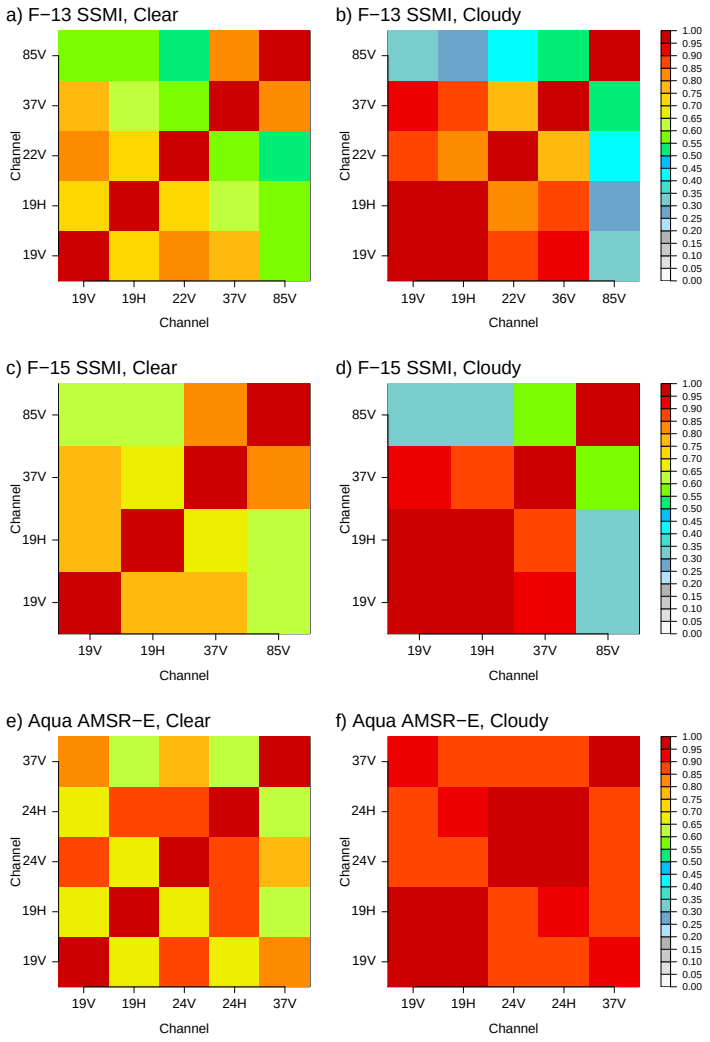

Figure 2: a) Estimates of inter-channel error correlations for the F13 SSM/I in clear conditions. b) As a), but for the cloudy sample. c, d) As a) and b), respectively, but for the F15 SSM/I. e, f) As a) and b), respectively, but for AMSR-E on Aqua.

The estimates of the observation errors are considerably smaller than the assumed observation error used in the assimilation system (cf Tables 1 and 2). The observation errors used are situation dependent, following Geer and Bauer (2011). The observation error model has been derived on the basis of FG-departures only, assuming that the background error is small (1 K). This results in relatively large observation errors, reflecting a cautious approach to the assimilation of the microwave imager data.

Inter-channel observation error correlations as estimated by the Desroziers diagnostic are shown in Fig. 2. Two aspects are striking: firstly, for the clear sample, all channels exhibit significant error correlations that are generally above 0.5 and frequently much higher than that. The finding is consistent with significant error correlations found for humidity-sounding instruments in Bormann and Bauer (2010). Secondly, for the 19-37 GHz channels, the cloudy class exhibits even stronger inter-channel error correlations which are generally above 0.7. In particular, the vertically and horizontally polarised channels of the same frequency have error correlations above 0.9 for this class, reflecting the de-polarisation effect of clouds and rain. In contrast, the 85 GHz channel on SSM/I is slightly less correlated with the other channels in the cloudy class than in the clear class, probably reflecting the different sensitivity to

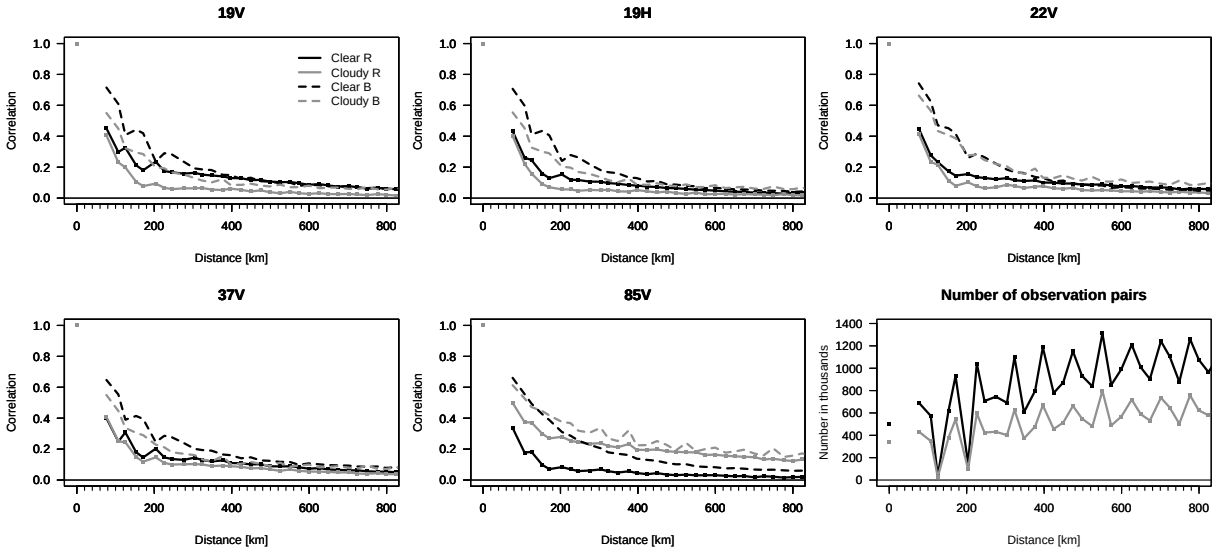

Figure 3: Estimates of spatial error correlations for the F13 SSM/I from the Desroziers diagnostic. Estimates of the observation error correlations are shown as solid lines, whereas those for the background error correlations are shown as dashed lines, with the clear sample shown in black and the cloudy sample shown in grey. The last panel gives the number of observation pairs (in thousands) that the estimates are based on. The highly variable number of observation pairs is due to the thinning/super-obbing applied to the data prior to the assimilation which averages observations to the T255 Gaussian grid.

ice-hydrometeors between these frequencies.

Next we will investigate spatial observation error correlations. To estimate these, we generated a database of pairs of FOVs for the respective instruments. All observations from the same orbit were matched up with each other, making sure that each observation pair is represented only once. The observation pairs were binned by separation distance in order to calculate isotropic error correlations with the Desroziers diagnostic (1). The binning interval used was 25 km.

Estimates of spatial error correlations of the F13 SSM/I are shown in Fig. 3. The results for equivalent channels for the other instruments are similar and are therefore not shown here. All channels show observation error correlations of around 0.2 or higher for separations of less than 100 km. For the 85V channel, the spatial observation error correlation for the cloudy class are broadest and considerably broader than their clear counterparts, reaching 0.2 only at around 400 km. For the 19-37 GHz channels, the clear class tends to exhibit slightly larger spatial observation error correlations than the cloudy class.

3.2 Single-FOV assimilation experiments

Given the strong inter-channel error correlations, particularly in the cloudy class, we will now investigate how the filtering properties of the assimilation system are affected by neglecting these or accounting for them. We will do this for the example of the cloudy class from the F-13 SSM/I; similar results would be obtained for the other instruments.

As a first step, it is useful to inspect the eigenvectors and eigenvalues of the error correlation matrix presented in Fig. 2b (e.g., Daley 1993; see Fig. 4). Normalised with the σ_os and projected onto these eigenvectors, the errors in the SSM/I observations will all be independent. For each eigenvector, the square root of the eigenvalues gives a measure of how the errors associated with that eigenvector are

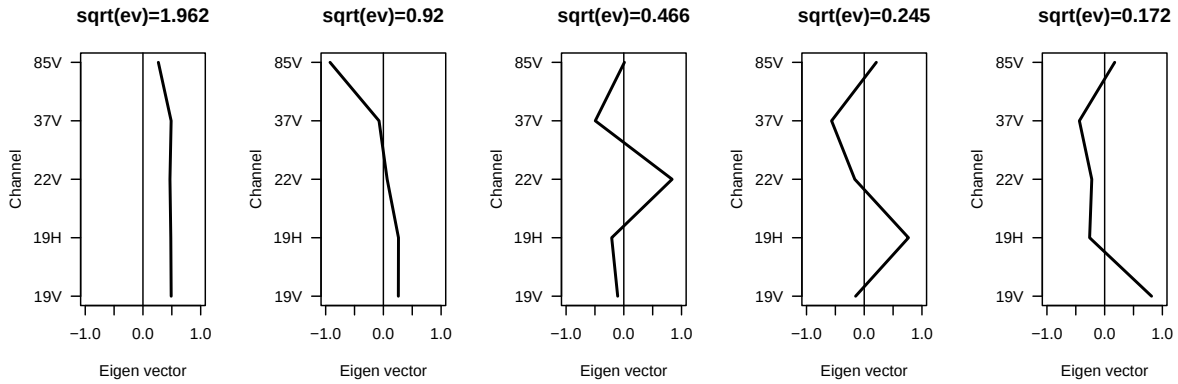

Figure 4: Eigenvectors of the error correlation matrix shown in Fig. 2b. Also given are the square roots of the associated eigenvalues above each pannel.

inflated or deflated relative to a diagonal matrix (cf Bormann et al. 2003 for a discussion of the spatial equivalent). We can see that in the case of correlated observation error, mean-like structures associated with the leading eigenvector will show a larger error compared to when the error covariance is diagonal (square root of the eigenvalue of $1.962 > 1$). In contrast, structures associated with higher-order eigenvectors instead show a smaller error, with eigenvalues of less than 1. As a result, if inter-channel observation error correlations are taken into account in an assimilation system, we can expect to see a situation-dependent down- or up-weighting of the observations compared to using a diagonal matrix, depending on whether the σ_o-normalised observation departures primarily project onto the leading or the higher eigenvectors.

The behaviour of up- or down-weighting the observations can be demonstrated in assimilation experiments. To highlight this, we perform assimilation experiments in which only a single selected SSM/I FOV is assimilated; all other observations are excluded. In the control experiment we use a diagonal observation error covariance matrix, whereas in the error-correlation experiment we explicitly take the inter-channel error correlations into account. The observation error (σ_o) and all other aspects are the same for both experiments. We study two cases here, both of them diagnosed as cloudy in the observations and the FG. The locations are 8.8N, 46.4W for case 1, and 29.1S, 44.2W for case 2, taken on 11 and 14 July 2009, respectively, with observation times close to the beginning of the 12Z 4DVAR assimilation window.

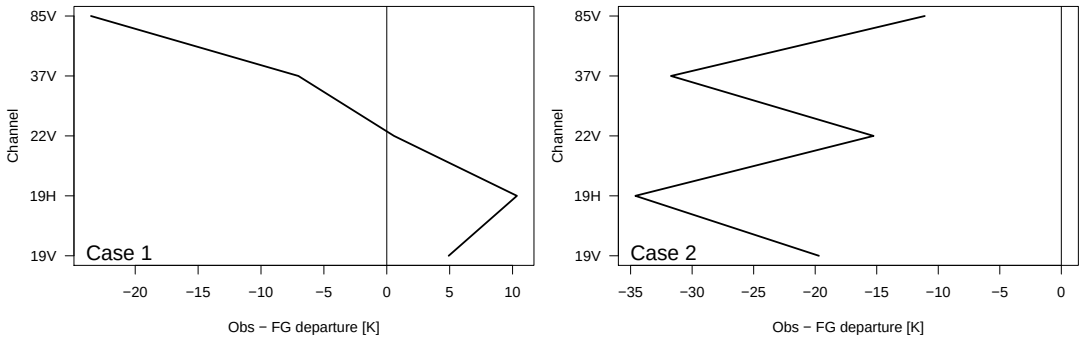

Figure 5: First guess departures (observation minus FG) [K] for the F13 SSM/I channels used in the ECMWF system for case 1 (left) and case 2 (right).

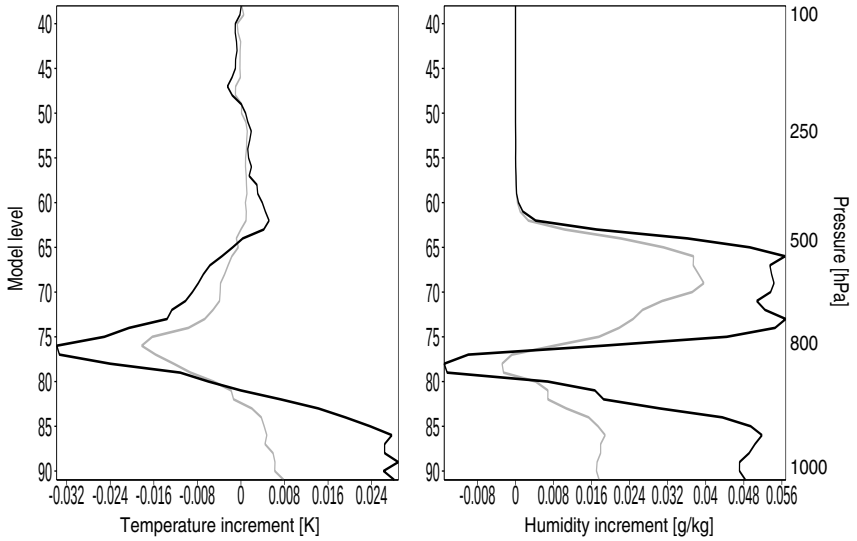

Figure 6: Vertical profile of the increments (analysis minus FG) for case 1 of the single-FOV experiments in terms of temperature (left) and humidity (right), valid at the beginning of the assimilation window. The increment profile has been extracted at the observation location. Grey indicates the results for a diagonal observation error covariance matrix, whereas black gives the results with inter-channel error correlations taken into account.

First Guess departures for the two cases are shown in Fig. 5. Case 1 shows FG departures with differing signs for different channels; once normalised by σ_o these project primarily onto the 2nd and 4th eigenvector of the error correlation matrix, associated with eigenvalues of less than 1. In contrast, case 2 shows FG departures consistently smaller than -10 K for all channels, projecting well onto the leading eigenvector after normalisation with σ_o.

As a result, taking the error correlations explicitly into account in the assimilation leads to larger increments for case 1 (Fig. 6), as the observations are receiving more weight. The increments are the difference between the analysis and the FG and therefore a measure of how strongly the observation affects the analysis. In contrast, case 2 exhibits smaller increments in the error correlation experiments (Fig. 7), as the inter-channel error correlations act to reduce the weight of the observations. The findings illustrate how taking observation error correlations into account in the assimilation can act to increase as well as decrease the weight of the observations.

4 Conclusions

In the present study we have estimated observation errors and their spatial and inter-channel error correlations for microwave imager radiances in the ECMWF system, and highlighted how inter-channel error correlations can alter the filtering properties of a 4DVAR assimilation system. The main findings are:

- The Desroziers diagnostic indicates larger observation errors for microwave imager data in cloudy regions, as would be expected due to larger observation operator and representativeness errors.
- Estimates for inter-channel error correlations are rather large for all three instruments, particularly for the 19-37 GHz channels in the cloudy class, for which error correlations are generally above 0.7. For the cloudy class, channels with the same frequency but different polarisations show particularly strong correlations exceeding 0.9, suggesting that errors arising from the cloud parameterisation (either in the moist physics or in the radiative transfer) dominate in these cases.

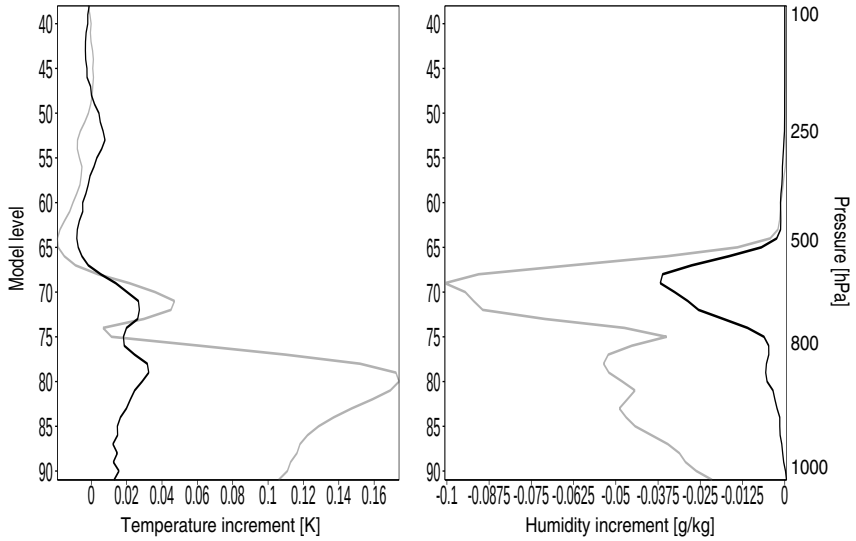

Figure 7: As Fig. 6, but for case 2.

- Considerable spatial error correlations can be found for separations of less than 100 km for all channels. The 85 GHz channel in cloudy conditions shows the broadest spatial error correlations, reaching 0.2 at around 400 km. Note, in the experiments used here, the data is super-obbed to T255 (≈80 km) resolution.
- Taking the inter-channel error correlations into account in the assimilation system can increase as well as decrease the weight given to the observations relative to assuming a diagonal error correlation matrix.

The present results are consistent with the findings for water vapour and window radiances in our earlier study (Bormann and Bauer 2010, Bormann et al. 2010). We again find considerable spatial and inter-channel error correlations for these channels, and a σ_o that is significantly larger than the measured instrument noise. This suggests that a large proportion of the observation error originates from the observation operator or from errors of representativeness. It is worth noting here that in strong-constraint 4DVAR the observation operator effectively includes the integration of the forecast model up to the observing time. These errors will inherently lead to inter-channel as well as spatial error correlations.

The findings of significant error correlations for the microwave imager radiances, especially in cloudy conditions, prompts the question what implications these have for the assimilation of the data within the current assumptions of variational data assimilation systems. One way to address the error correlations could be to revise the spatial thinning or the channel selection, while continuing to use a diagonal observation error covariance matrix. This is the most cautious option, and it is likely to also reduce the effect of limitations due to the assumption of uncorrelated background and forward model error made in today's assimilation systems. Alternatively, observation error correlations could be included explicitly in the assimilation system. Our single-FOV assimilation experiments demonstrate that accounting for these can increase as well as decrease the weight of the observations, suggesting that an accurate specification of these inter-channel error correlations is likely to be important.

Acknowledgements

The assimilation experiments with inter-channel error correlations used software originally developed by Andrew Collard. Alan Geer was funded by the EUMETSAT fellowship programme.

References

Bauer, P., A. Geer, P. Lopez, and D. Salmond, 2010: Direct 4D-Var assimilation of all-sky radiances. Part I: Implementation. *Q. J. R. Meteorol. Soc.*, **136**, 1868–1885.

Bormann, N., and P. Bauer, 2010: Estimates of spatial and inter-channel observation error characteristics for current sounder radiances for NWP, part I: Methods and application to ATOVS data. *Q. J. R. Meteorol. Soc.*, **136**, 1036–1050.

Bormann, N., A. Collard, and P. Bauer, 2010: Estimates of spatial and inter-channel observation error characteristics for current sounder radiances for NWP, part II: Application to AIRS and IASI. *Q. J. R. Meteorol. Soc.*, **136**, 1051–1063.

Bormann, N., A. Geer, and P. Bauer, 2011: Estimates of observation error characteristics in clear and cloudy regions for microwave imager radiances from NWP. *Q. J. R. Meteorol. Soc.*, **137**, accepted.

Bormann, N., S. Saarinen, G. Kelly, and J.-N. Thépaut, 2003: The spatial structure of observation errors in Atmospheric Motion Vectors from geostationary satellite data. *Mon. Wea. Rev.*, **131**, 706–718.

Daley, R., 1993: *Atmospheric data analysis*. Cambridge University Press, Cambridge, UK, 460 pp.

Dee, D., 2004: Variational bias correction of radiance data in the ECMWF system. In ECMWF Workshop on Assimilation of High Spectral Resolution Sounders in NWP, ECMWF, Reading, UK, 97–112.

Dee, D., and A. da Silva, 1999: Maximum-likelihood estimation of forecast and observation error covariance parameters. Part I: Methodology. *Mon. Wea. Rev.*, **127**, 1822–1834.

Desroziers, G., L. Berre, B. Chapnik, and P. Poli, 2005: Diagnosis of observation, background and analysis-error statistics in observation space. *Q. J. R. Meteorol. Soc.*, **131**, 3385–3396.

Geer, A., and P. Bauer, 2010: Enhanced use of all-sky microwave observations sensitive to water vapour, cloud and precipitation. Technical Memorandum 620, ECMWF, Reading, UK, 41 pp [available under www.ecmwf.int/publications/library/ecpublications /_pdf/tm/601–700/tm620.pdf].

Geer, A., and P. Bauer, 2011: Observation errors in all-sky data assimilation. *Q. J. R. Meteorol. Soc.*, **137**, accepted.

Geer, A., P. Bauer, and P. Lopez, 2010: Direct 4D-Var assimilation of all-sky radiances. Part II: Assessment. *Q. J. R. Meteorol. Soc.*, **136**, 1886–1905.

Hollinger, J., J. Peirce, and G. Poe, 1990: SSM/I instrument evaluation. *IEEE Trans. Geosci. Remote Sens.*, **28**, 781–790.

Hollingsworth, A., and P. Lönnberg, 1986: The statistical structure of short-range forecast errors as determined from radiosonde data. Part I: The wind field. *Tellus*, **38A**, 111–136.

Kawanishi, T., T. Sezai, Y. Ito, K. Imaoka, T. Takeshima, Y. Ishido, A. Shibata, M. Miura, H. Inahata, and R. Spencer, 2003: The Advanced Microwave Scanning Radiometer for the Earth Observing System (amsr-e), NASDA's contribution to the EOS for global energy and water cycle studies. *IEEE Trans. Geosci. Remote Sens.*, **41**, 184–194.

Rabier, F., H. Järvinen, E. Klinker, J.-F. Mahfouf, and A. Simmons, 2000: The ECMWF operational implementation of four-dimensional variational assimilation. Part I: Experimental results with simplified physics. *Q. J. R. Meteorol. Soc.*, **126**, 1143–1170.

Rutherford, I. D., 1972: Data assimilation by statistical interpolation of forecast error fields. *J. Atmos. Sci.*, **29**, 809–815.